

**Degradation of N-methyl 2-pyrrolidone through
advanced oxidation process in presence of bismuth-
based heterogenous catalysts**

A project

submitted in partial fulfilment of the requirement

for the award of degree of

Bachelor in Technology

.....Chemical Engineering.....

Submitted by

Miquel Molina Garcia

Home university

Universitat Politecnica de Valencia (Spain)

Under the Guidance of

Faculty coordinator:

Prof. Dr. Urška Lavrenčič Štangar

2nd faculty coordinator:

Dr. Praveen Kumar

Univerza v Ljubljani



**Faculty of Chemistry and Chemical Technology, University of Ljubljana, Večna
pot 113, 1000 Ljubljana, Slovenia**

Abstract

This study investigates the degradation of N-methyl-2-pyrrolidone (NMP) by UV-C and UV-C/PMS-treatment processes. The degradation of NMP was less than 2% by UV-C photolysis. To enhance the degradation of NMP, zinc and molybdenum-based photocatalysts were synthesized and investigated. Several photocatalysts based on Bi-ZnMoO₄ were successfully synthesized by a modified hydrothermal method. These photocatalysts had different molar ratios of bismuth with respect to ZnMoO₄ (molar ratios 10, 20 and 30%). The synthesized photocatalysts were characterized by various techniques such as XRD and BET to decipher their structural and surface properties. To enhance the degradation, PMS was used as a source of sulfate (SO₄^{•-}) and hydroxyl (HO[•]) radicals in the UV-C photolysis treatment system. UV radiation is used as a source to activate the PMS for sulfate and hydroxyl radical generation. The operational parameters such as initial pH and concentration of NMP and PMS were studied to understand their effects on degradation.

Keywords: NMP degradation, photocatalyst, hydrothermal process, PMS, ZnMoO₄, Bi₂MoO₆

Index

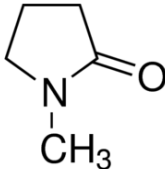
1. Introduction-----	Page 3
1.1 N-methyl-2-pyrrolidone-----	Page 3
1.2 Advanced oxidation processes-----	Page 4
1.3 Peroxymonosulfate-----	Page 5
1.4 Photocatalysts based on Bi and Zn-----	Page 7
2. Objectives of the study-----	Page 9
3. Materials and methods-----	Page 10
3.1 Chemicals-----	Page 10
3.2 Analytical instruments-----	Page 10
3.3 Synthesis of Bi ₂ MoO ₆ / ZnMoO ₄ -----	Page 10
3.4 Characterization techniques-----	Page 11
3.5 Reactions and analysis of photocatalytic activity-----	Page 12
4. Results and discussions-----	Page 13
4.1 Results of XRD characterization-----	Page 13
4.2 Results of BET characterization-----	Page 14
4.3 Effect of concentration of PMS-----	Page 15
4.4 Comparison of the effect of PMS concentration for each catalyst-----	Page 18
4.5 Effect of initial pH-----	Page 19
4.6 Effect of NMP concentration-----	Page 20
4.7 Effect of UV light-----	Page 20
5. Conclusions-----	Page 21
6. References-----	Page 21

1. Introduction

1.1. N-Methyl-2-Pyrrolidone (NMP)

N-Methyl-2-Pyrrolidone (NMP) is a 5-membered cyclic amide, with a carbonyl and a methyl group. It is a colorless liquid. The various characteristics are provided in Table 1.

Table 1. Characteristics of N-methyl-2-pyrrolidone. Source: datasheet of NMP [1]

Molecular formula	C ₅ H ₉ NO
Density	1.03 g/ cm ³
Molecular weight	99.133 g/ mol
Water solubility	Completely soluble
Chemical structure	

It can cause skin, eyes and respiratory irritation, as well as damage to the unborn child. Thus, pregnant women must not work with this chemical, and full-body protection and glasses must be used when working with it [1].

NMP is produced through an ester-to-amide conversion, using methylamine to convert butyrolactone to NMP. Industrial production is estimated to be around 20000-30000 tons annually.

It is widely used in industry as a solvent, in electronic, petrochemical TFC-LCD manufacturing, agrochemical, pharmaceutical industry and in the production of industrial cleaners, paints, and coatings [2].

However, its healthy and environmental risks have made investigators and industries use more harmless solvents to replace NMP. NMP presents several risks to human health, such as for the reproductive system, liver, kidney, immunological and developmental systems and central neurological system. Its use to produce lithium-ion batteries is decreasing, as water can also be used [3].

In the European Union, NMP is subject to restrictions and control under REACH (Registration, Evaluation, Authorisation and Restriction of Chemicals) regulation. The Long-Term Exposure Limit (LTEL) values are 40 mg/m³ and 10 ppm, while the Short-Term Exposure Limit (STEL) values are 80 mg/m³ and 20 ppm [4].

Some authors have proved that biological treatment is highly efficient against NMP, with the use of bacteria such as *Paracoccus*, *Mesorhizobium*, *Pseudomonas*, *Rhizobium*, *Acinetobacter*, *Rhodococcus*, *Alicyclophilus*, *Patulibacter* and *Rhodococcus genera* [5][6][7]. However, this is a very slow process and produces a carbonyl

molecule with a high COD that cannot be degraded under conventional treatment processes [8].

1.2. Advanced oxidation processes

Due to the high toxicity, polymeric structures, and non-biodegradable characteristics of some pollutants, traditional biological treatment for wastewater treatment plants (WWTP) are useless [9]. Also, some widely used physical (filtration, flotation) and chemical (coagulation-flocculation) treatments produce high quantities of solid waste and contaminants. As an efficient water treatment technology, chemical methods can rapidly oxidize and completely degrade organic pollutants. Among various chemical methods, advanced oxidation processes (AOPs) are rightfully considered to be the best method for treating organic wastewater containing micropollutants. High mineralization efficiency, rapid oxidation reaction rate and no secondary pollution are the advantages of AOPs. AOPs, including Fenton reactions, photocatalytic oxidation, electrochemical oxidation reactions, sonochemical oxidation, sulfate radical-based AOPs (SR-AOPs), etc., can fully degrade the pollutant.

Their main goal is to fully oxidize the organic pollutant through the generation of highly active radicals. [10] These radicals include hydroxyl (HO^\bullet), superoxide ($\text{O}_2^{\bullet-}$) and sulfates ($\text{SO}_4^{\bullet-}$).

Hydroxyl radical has a redox potential of 2.8 V, being the fluorine the only known species with a higher potential (Table 2). However, its use as an oxidant is limited to a pH range of 2-4, and, also, H_2O_2 is very unstable. Sulfate radical has a standard reduction potential of 2.07 V, lower than that of hydroxyl radical, but, on the other hand, can work in a pH range of 2-8, and shows a longer lifetime [11].

Table 2. The standard reduction potential of selected oxidant species (Loures et al. [12])

Species	E° (V, 25 °C)
Fluorine (F_2)	3.03
Hydroxyl radical (HO^\bullet)	2.80
Atomic oxygen (O_2)	2.42
Ozone (O_3)	2.07
Hydrogen peroxide (H_2O_2)	1.78
Perhydroxyl radical (HO_2^\bullet)	1.70
Hypochlorous acid (HClO)	1.49
Chlorine (Cl_2)	1.36
Bromine (Br_2)	1.09
Iodine (I_2)	0.54

AOP systems present several advantages [12]:

- Some AOP can produce the complete mineralization (conversion of organic compounds in CO₂, H₂O, and inorganic acids...) of the pollutants.
- They can destroy or convert the refractory compounds that cannot be treated by biological methods.
- They can convert the recalcitrant compounds that come from biodegradation processes.
- Strong oxidants are used, so the reactions have high reaction rates.
- They can be used to treat the compounds that originate from another pre-treatment, for example, disinfection by chlorine.
- If the optimum quantity of reactant is used, then the formation of by-products will be minimal.
- They enable *in situ* treatment.

However, AOP also shows some disadvantages and limits, so it cannot be arbitrarily used [12]:

- Not all processes can be used on an industrial scale.
- Specially in processes using UV, the energetic cost might be high.
- In some cases, like the Fenton process, the oxidant concentration must be strictly controlled, as well as pH, especially if it is a post-treatment.

1.3. Peroxymonosulfate (PMS)

Sulfate radicals are usually obtained via the activation of peroxymonosulfate (PMS) (Fig. 1) or persulfate S₂O₈²⁻ (PS). They can be activated through heating [11], UV or transition metals (Fe²⁺, Co²⁺, Ag⁺) [13]. In Table 3 there is a brief summary of these methods.



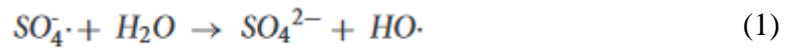
Figure 1: PMS and photocatalyst used during the experiments.

Table 3: Summary of the different PS and PMS activation approaches (Xia et al. [14])

Method	Reaction	Mechanism	Key parameter
UV	$S_2O_8^{2-} + hv \rightarrow 2SO_4^{\cdot-} \cdot (PS)$ $HSO_5^- + hv \rightarrow SO_4^{\cdot-} \cdot + OH \cdot (PMS)$	Fission of O-O bond	UV under 254 nm wavelength [24]
Heating	$S_2O_8^{2-} + heat \rightarrow 2SO_4^{\cdot-} \cdot (PS)$ $HSO_5^- + heat \rightarrow SO_4^{\cdot-} \cdot + OH \cdot (PMS)$	Fission of O-O bond	Higher temperatures can cause side effects. Very expensive in terms of energy.
Transition metal	$S_2O_8^{2-} + M^{n+} \rightarrow M^{n+1} + SO_4^{2-} + SO_4^{\cdot-} \cdot (PS)$ $HSO_5^- + M^{n+} \rightarrow M^{n+1} + SO_4^{\cdot-} \cdot + OH \cdot (PMS)$	Single electron transfer	Homogeneous catalysts are cheaper than a heterogeneous catalyst

For the activation through heating, an energy input of 140-213.3 kJ/mol is necessary for a temperature above 50°C [15]. And Yang et al. (2010) [16] showed that the oxidation efficiency of PS is higher than that of PMS, due to the higher bond energy of the O-O in the PMS.

For the activation through UV, two sulfate radicals are obtained from PS, and sulfate and hydroxyl from PMS, as it happens with heating. However, Chen et al. (2019) [17] found that, for acidic pH, sulfate is the predominant radical, while, for pH > 9.3, sulfate radical reacts with water to form hydroxyl radical, as it's shown in equation (1).



PS and PMS can be also activated through transition metals like Fe, Co, Ag and Mn, thanks to the transfer of an electron. However, the main issue of this method is that these metals can't be used in high concentrations, as it can cause environmental problems. That's why several authors, like Shi et al. (2012) [18] have used some catalysts like graphene, activated carbon or metal oxides to reduce the loading of these metals.

Several authors [19][20][21] studied the effectiveness of several AOPs methods for the degradation of BPA (Bisphenol A).

These methods were UV, UV/H₂O₂, UV/K₂S₂O₈ or UV/Na₂CO₃, and the radicals produced by these methods were OH· (for H₂O₂), SO₄^{•-} (for K₂S₂O₈) and CO₃^{•-}/HCO₃^{•-} (for Na₂CO₃). The best results were obtained for the UV/K₂S₂O₈ system, which produces the same radical as the PMS, with a BPA removal of 95%.

Several factors affect the degradation efficiency, such as temperature, pH, catalyst loading and concentration of PS/PMS. Shi et al. (2019) [18] found that, for a concentration of 35 mM of PS, it was possible to remove 99% of BPA, while Feng et al. (2017) [22] got a removal of 100% of ketoprofen with a pH of 10.

1.4. Photocatalysts based on Zn and Bi

In order to increase the efficiency of the UV/oxidant treatment, Kumar et al. [23] thought about using a photocatalyst alongside with PMS. A typical semiconductor like TiO₂ was one of the first candidates, as it is not toxic, is cheap, has high reactivity and is stable. However, it can only be activated by UV light, meaning that the optical frequency response range is narrow. Also, TiO₂ has four polymorphs: orthorhombic brookite, tetragonal anatase, tetragonal rutile and monoclinic TiO₂ (B), and each one is suitable for different types of reactions [24]. These factors made the authors [23] search for another photocatalyst with better optical and chemical properties.

Metal tungstates of the form MWO₄ have gained the attention of several authors in recent years. ZnWO₄ has shown high photoactivity under UV irradiation, and Bi₂WO₆ shows photoactivity not only under UV but also under visible light. By combining two or more photocatalysts is possible to improve their characteristics (an increase in charge separation and charge transfer at the interface or an increase in the lifespan of the charge carriers) [25].

Hojamberdiev et al. [25] proposed a one-step strategy for the preparation of ZnWO₄/Bi₂WO₆ catalyst by hydrothermal processing, and the resultant photocatalyst was studied by using it for the degradation of acetaldehyde under UV light irradiation. Several ratios of both compounds were analyzed, as well as the pure catalysts. Table 3 shows the results of the degradation of acetaldehyde into CO₂ after 6 hours of UV irradiation.

Table 3: Results of Hojamberdiev et al. [25] experiments.

Photocatalyst	Conversion of AcH (%)
Pure ZnWO ₄	36.2
Pure Bi ₂ WO ₆	44
5% Bi ₂ WO ₆ / ZnWO ₄	52.8
10% Bi ₂ WO ₆ / ZnWO ₄	60.8
15% Bi ₂ WO ₆ / ZnWO ₄	71.2
20% Bi ₂ WO ₆ / ZnWO ₄	79.8

25% Bi ₂ WO ₆ / ZnWO ₄	86.2
30% Bi ₂ WO ₆ / ZnWO ₄	100

This proves that the composite photocatalyst shows much better activity than the pure compounds, as it is possible to reach a 100% conversion for a 30% ratio of Bi₂WO₆/ ZnWO₄. Also, they found that this reaction follows a first-order reaction, and its constant increases with the content of Bi₂WO₆ in the composite, meaning the reaction is the fastest with 30% Bi₂WO₆/ZnWO₄.

Kumar et al. [23] synthesized the same catalyst but with a modified hydrothermal method, and also studied the influence of pH and the hydrothermal synthesis time on the photocatalytic and optical properties of the photocatalysts obtained.

They tested the removal of Plasmocorinth B dye with pure ZnWO₄, pure Bi₂WO₆ and with different ratios of Bi₂WO₆/ ZnWO₄, and they found that the removal was quite higher using the 30% Bi₂WO₆/ ZnWO₄ ratio (Fig. 2).

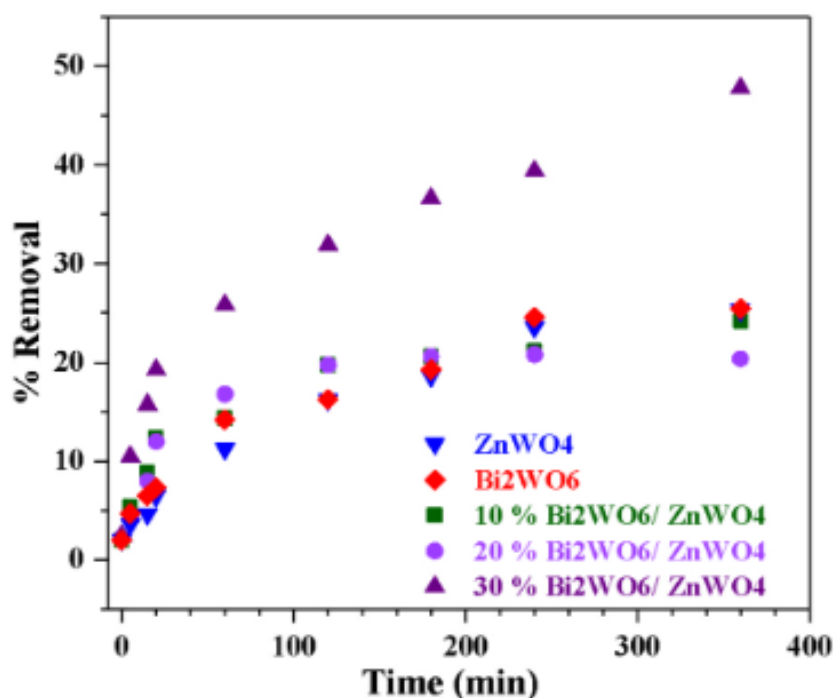


Figure 2: Plasmocorinth B dye degradation in the previous study [23].

Also, the characterization techniques used with the photocatalysts synthesized showed that the band gap was reduced, meaning that the photocatalytic activity has improved (Table 4).

Table 4: Band gap for the different photocatalysts obtained, Kumar et al. [23]

Compound	Band gap (eV)
ZnWO ₄	4.7
Bi ₂ WO ₆	3.9
10 % Bi ₂ WO ₆ / ZnWO ₄	3.7
20% Bi ₂ WO ₆ / ZnWO ₄	3.6
30% Bi ₂ WO ₆ / ZnWO ₄	3.5

2. Objectives of the study

N-Methyl-2-pyrrolidone (NMP) is a multipurpose solvent and reaction medium used in a variety of industries, namely electronics, petrochemical processing, TFT-LCD manufacturing units, agrochemicals, pharmaceuticals, industrial cleaners, paints, and coatings. NMP has been linked to a multitude of human health risks, including impacts on the reproductive system, liver, kidney, immunological system, developmental system and central neurological systems. Due to these harmful effects on humans, NMP has been subject to regulation in European Union countries under REACH. The US EPA has also listed the NMP in Candidate Contamination List (CCL) 3 and 4. The biological wastewater treatment processes have shown effectiveness in NMP removal. The biodegradation of NMP, on the other hand, is not only slow but also produces a carbonyl molecule with a high COD that cannot be degraded further under conventional treatment processes. These limitations have led to the rapid research in the discipline of advanced oxidation processes (AOPs) for the degradation of recalcitrant chemicals.

AOPs have been shown to be excellent treatment methods for removing NMP from water. Ozone, UV irradiation, and the hydroxyl radical are inefficient in ordinary water treatment plant conditions. In recent years, sulfate radical-based advanced oxidations processes (AOPs) in treating emerging pollutants have gained researchers' attention. The formation of degradation by-products (DBP) is a major concern both in biological and chemical oxidation processes. Sometimes these DBPs are found to be more harmful than the parent compound. Therefore, the present study will focus on

- Degradation of the NMP below the statutory levels and reducing the toxicity to the desired level.
- Synthesis of various bismuth-based photocatalysts.
- Various sulfate radical generating oxidants will also be explored with developed photocatalysts.

- Effect of various operating parameters such as pH, exposure time to irradiation, catalyst dosage, cations, anions, and the natural organic matter on the degradation of NMP shall be investigated.

The insights gained through this project might be helpful to improve the quality of drinking water in the distribution system. This project may also be informative for the industries to improve the quality of the effluent before the discharge.

3. Materials and methods

3.1. Chemicals

NMP (+99%) was purchased from Alfa Aesar, methanol was supplied by Sigma Aldrich (99.9%), while potassium peroxymonosulfate (PMS, extra pure, 4.5% active oxygen) was from Acros Organics. For the synthesis of the photocatalysts, zinc nitrate hexahydrate ($\text{Zn}(\text{NO}_3)_2 \cdot 6\text{H}_2\text{O}$) was supplied from Fisher Chemicals, sodium molybdenum oxide dihydrate ($\text{Na}_2\text{MoO}_4 \cdot 2\text{H}_2\text{O}$ 98%) from Alfa Aesar, and bismuth (III) nitrate pentahydrate ($\text{Bi}(\text{NO}_3)_3 \cdot 5\text{H}_2\text{O}$ 98%) was from Sigma Aldrich.

3.2. Analytical instruments

NMP containing solutions and HPLC mobile phase were prepared using a Milli-Q water system (Millipore, Bedford, USA). NMP was quantified by HPLC (Agilent Scientific Instruments, model 1260 Infinity II) using a PDA detector at a wavelength of 214 nm. HPLC was operated in an isocratic mode at 25 °C temperature with a mobile phase at a flow rate of 0.7 mL/min. The mobile phase was composed of 5% acetonitrile and 95% Milli-Q water. The limit of detection (LOD) for NMP was found to be 0.14 mg/L. The total organic carbon (TOC) was measured through TOC 5000A, Shimadzu.

3.3. Synthesis of Bi_2MoO_6 / ZnMoO_4

Kumar et al. [23] synthesized pure ZnWO_4 and Bi_2WO_6 , as well as mixed compounds of these chemicals with different molar ratios (Bi_2WO_6 / ZnWO_4 0.1-0.2-0.3), using a hydrothermal technique. The same technique and methods were used in this work to prepare the Bi_2MoO_6 / ZnMoO_4 photocatalyst.

The chemicals used were $\text{Zn}(\text{NO}_3)_2 \cdot 6\text{H}_2\text{O}$ ($M_w = 297.46$ g/mol); $\text{Bi}(\text{NO}_3)_3 \cdot 5\text{H}_2\text{O}$ ($M_w = 484.99$ g/mol) and $\text{Na}_2\text{MoO}_4 \cdot 2\text{H}_2\text{O}$ ($M_w = 241.95$ g/mol).

To prepare the pure ZnMoO_4 , 7.5 mmol of $\text{Zn}(\text{NO}_3)_2 \cdot 6\text{H}_2\text{O}$ were weighed, as well as 7.5 mmol of $\text{Na}_2\text{MoO}_4 \cdot 2\text{H}_2\text{O}$. These quantities were added to 60 mL of deionized water and 15 mL of ethyleneglycol at room temperature under vigorous stirring (500 rpm). Then, with 25% ammonia solution, the pH was adjusted to 9, and after 1 hour of continuous stirring, a white solution was obtained.

This solution was put in several 50 mL Teflon autoclaves and in the oven at 180°C for 24 hours. (Fig. 3)



Figure 3: A) Teflon liners, B) autoclaves used for the synthesis. C) Oven used for hydrothermal process

After the autoclave was taken out of the oven and cooled down, the resultant suspension was subjected to vacuum filtration to separate the liquid from the photocatalyst, which was weighed and placed in a small vessel.

The same procedure was followed to obtain pure Bi_2MoO_6 and the different combinations of these two compounds. Table 5 shows the quantities used and obtained.

Table 5: Quantities of each chemical used for the synthesis of the catalysts and quantities of the products obtained

Catalyst	$\text{Zn}(\text{NO}_3)_2$ mmol	Na_2MoO_4 mmol	$\text{Bi}(\text{NO}_3)_3$ mmol	$\text{Zn}(\text{NO}_3)_2$ mg	Na_2MoO_4 mg	$\text{Bi}(\text{NO}_3)_3$ mg	Obtained mg
ZnMoO_4	7.5	7.5	-	2230.95	1815	-	1008.3
Bi_2MoO_6	-	7.5	7.5	-	1815	3637.5	2137.9
10% $\text{Bi}_2\text{MoO}_6/\text{ZnMoO}_4$	7.5	7.5	0.75	2230.95	1815	363.75	1313
20% $\text{Bi}_2\text{MoO}_6/\text{ZnMoO}_4$	7.5	7.5	1.5	2230.95	1815	727.5	1405
30% $\text{Bi}_2\text{MoO}_6/\text{ZnMoO}_4$	5	5	1.5	1487.3	1209.75	727.5	1157.8

3.4. Characterization techniques

The synthesized $\text{Bi}_2\text{WO}_6/\text{ZnWO}_4$ was characterised by XRD for phase identification and crystallite size. XRD measurements were recorded employing a Siemens D5000 diffractometer over a range of $2\theta = 5^\circ\text{--}80^\circ$ with a step size of 0.02° at

40 kV with Cu-K α radiation ($\lambda = 0.15406$ nm). The average crystallite size was calculated from the recorded XRD pattern using the Scherrer equation.

Nitrogen adsorption and desorption isotherms with a multi-point method were performed by Micromeritics ASAP 2020 at -197 °C. The surface area of the catalysts was determined using the BET method and pore size distribution was estimated from the BJH method using the adsorption branch of the isotherms.

3.5. Reactions and analysis of photocatalytic activity

To measure the effectiveness of the photocatalyst on the degradation of NMP, several reactions were made. First of all, a stock solution of NMP with concentration of 10 mg/L was prepared. As NMP has a density of 1030 mg/mL, to prepare 1L of this solution 0.0097 mL of NMP was needed (Fig. 4a). This solution was vigorously stirred to be sure it was homogeneous.

The different reactions were made with different quantities of PMS, and with different catalysts. The quantity of NMP solution was fixed to 50 mL in every reaction (0.5 mg of NMP) and the proportion of NMP:PMS or NMP:catalyst was different for each reaction.

For a proportion of 1:10, 5 mg of PMS/ catalyst were used, for 1:20, 10 mg of each one were added, and for a proportion of 1:30, 15 mg were needed. The objective was to know which quantity of PMS and photocatalyst offer better results for the degradation of NMP.

The solutions were put in a UV reactor (Fig. 4b), for 3-4 hours. Every 15-30 minutes a sample of 0.8 mL was taken from the reaction (also before adding PMS and the photocatalyst, for $t = 0$). The samples were then put in a vial, along with 0.1 mL of methanol, used to stop the reaction.

Once all the samples of the reaction were taken, they were analyzed by HPLC (Fig. 4c).



Figure 4: A) NMP bottle used for the experiments. B) UV reactor used for the reactions. C) HPLC device used for the samples' analysis.

4. Results and discussion

4.1. Results of XRD characterization

XRD of the prepared pure Bi_2MoO_6 , ZnMoO_4 , and $\text{Bi}_2\text{MoO}_6/\text{ZnMoO}_4$ photocatalysts is shown in (Fig 5). Diffraction peaks in all photocatalysts are well-defined and sharp, indicating a high degree of structural order. The hydrothermal reaction temperature plays a vital role in crystal formation, as observed by the presence of narrower peaks with higher intensity. ZnMoO_4 and Bi_2MoO_6 are present as the main phases. As the molar ratio of $\text{Bi}_2\text{MoO}_6/\text{ZnMoO}_4$ was increased from 10% to 30%, the peak intensities of ZnMoO_4 decreased, while the intensity of the diffraction peaks of orthorhombic Bi_2MoO_6 increased.

In $\text{Bi}_2\text{MoO}_6/\text{ZnMoO}_4$ composites, there is no impurity peak, indicating that the composites are two-phase: ZnMoO_4 and Bi_2MoO_6 [23]. The diffraction peaks of the synthesized $\text{Bi}_2\text{MoO}_6/\text{ZnMoO}_4$ composites are very similar to those of pure Bi_2MoO_6 and ZnMoO_4 , but they broaden significantly compared to those of pure Bi_2MoO_6 and ZnMoO_4 . This implies that the final product may have smaller particles than one-phase analogues.

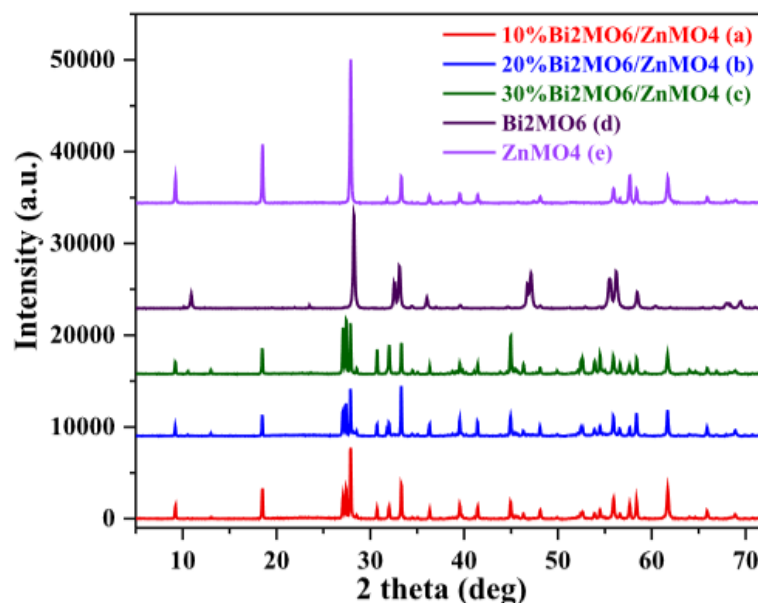


Figure 5: XRD of the synthesized photocatalysts

The small crystallite size correlates with a more effective redox ability [23]. The formation of bonds on the surface of $\text{Bi}_2\text{MoO}_6/\text{ZnMoO}_4$ composites may be responsible for the decrease in crystallite size. As a result, crystallite growth is inhibited. Moreover, the crystallite size decreases due to the difference between the ionic radii of Zn^{2+} (0.74 Å) and Bi^{3+} (1.03 Å). A similar inhibitory effect was also observed by Fifere et al. [26], Jaya-

chandraiah and Krishnaiah [27] and Sin et al. [28]. The microstrain in $\text{Bi}_2\text{MoO}_6/\text{ZnMoO}_4$ composite is higher compared to Bi_2MoO_6 and ZnMoO_4 . This indicates a crystalline structure distortion that is caused by changes in lattice parameters and a decrease in crystal size.

4.2. Results of BET characterization

The pore size and pore volume of the catalysts were calculated by the BJH method and the surface area of the catalysts was calculated using the BET method. The measurements of N_2 adsorption-desorption isotherm, cumulative pore volume with respect to pore diameter measurements for the $\text{Bi}_2\text{MoO}_6/\text{ZnMoO}_4$ catalysts are shown in (Fig 6); and the calculated values of the average pore diameter, pore volume and BET surface area are shown in Table 6.

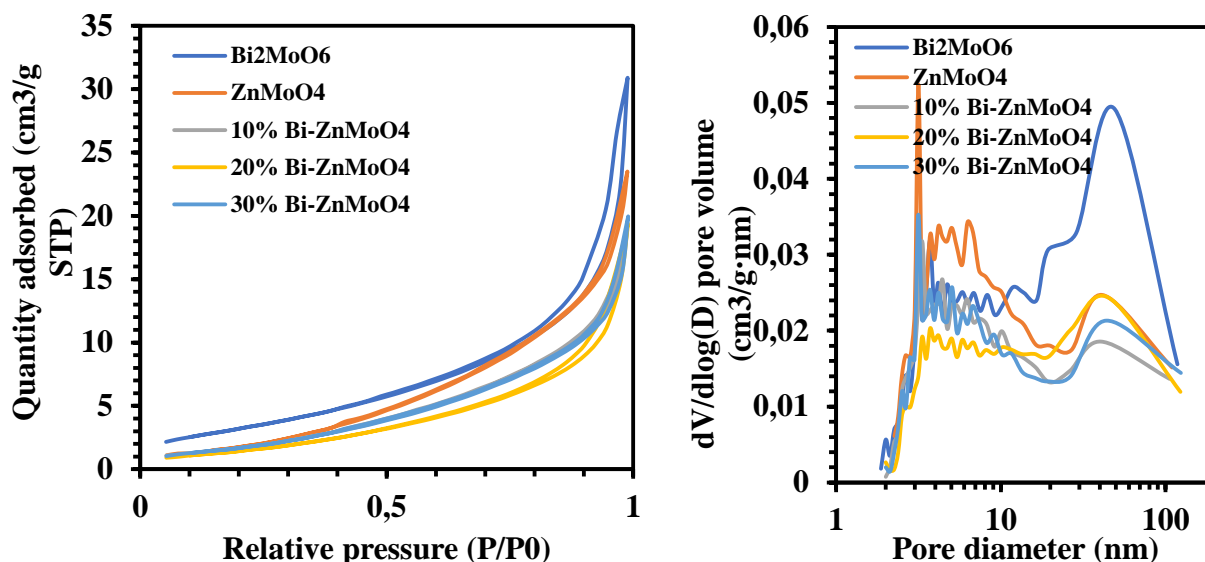


Figure 6: A) N_2 adsorption/ desorption isotherms. B) pore size distribution for $\text{Bi}_2\text{MoO}_6/\text{ZnMoO}_4$ catalysts

Table 6: Textural properties of the synthesized catalysts

Catalyst	Surface area (m^2/g)	Cumulative pore volume (cm^3/g)	Average pore diameter (nm)
ZnMoO_4	7.0	0.040	10.3
10% $\text{ZnMoO}_4/\text{Bi}_2\text{MoO}_6$	6.8	0.032	17.1
20% $\text{ZnMoO}_4/\text{Bi}_2\text{MoO}_6$	5.8	0.032	20.5
30% $\text{ZnMoO}_4/\text{Bi}_2\text{MoO}_6$	7.0	0.033	17.6

4.3. Effect of concentration of PMS

The main part of the study focuses on the influence of PMS concentration on NMP degradation. Several experiments were made with a fixed NMP concentration of 10 mg/L and catalyst concentration of 300 mg/L, while changing PMS concentration from 100 to 200 to 300 mg/L, and also experiments with each photocatalyst were made without using PMS at all.

Reactions without using PMS (only catalyst): without PMS, no remarkable catalytic activity was found for the mixed catalysts, and a maximum degradation of 25% was found for both ZnMoO₄ and Bi₂MoO₆. (Fig. 7)

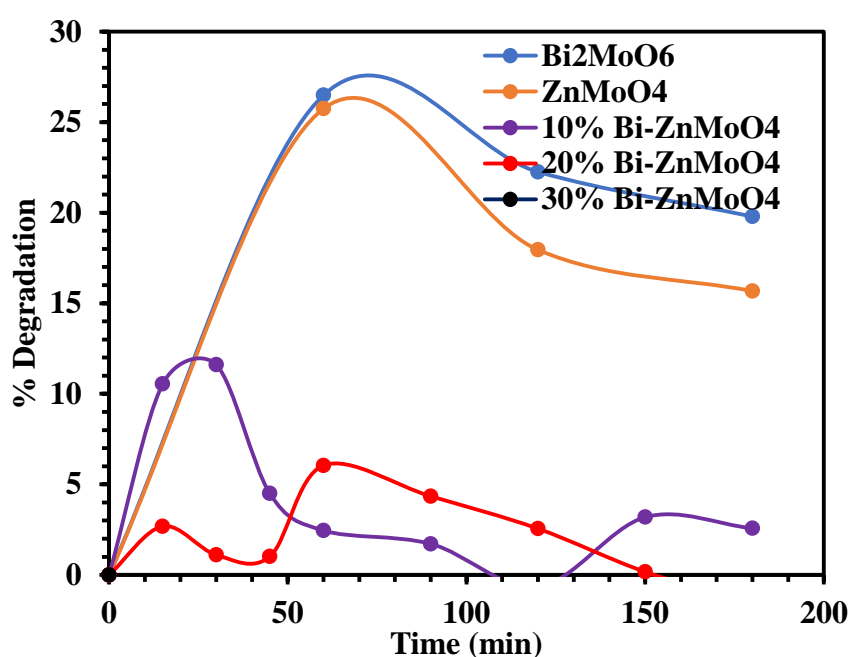


Figure 7: NMP degradation for experiments without PMS (NMP concentration 10 mg/L, catalyst loading 300 mg/L)

Reaction with PMS 100 mg/L: in this reaction 5 mg pf PMS were added to see the degradation of NMP. As shown in (Fig. 8) and Table 7, the best results were found for the pure catalysts, especially for Bi₂MoO₆, as a degradation of 70% was reached in only 2 hours.

Table 7. Degradation of NMP with 100 mg/L of PMS

Catalyst	Degradation after 4 hours
Bi ₂ MoO ₆	68.7%
ZnMoO ₄	65.3%
10% Bi ₂ MoO ₆ / ZnMoO ₄	36.2%
20% Bi ₂ MoO ₆ / ZnMoO ₄	34.4%

30% Bi ₂ MoO ₆ / ZnMoO ₄	27.9%
---	-------

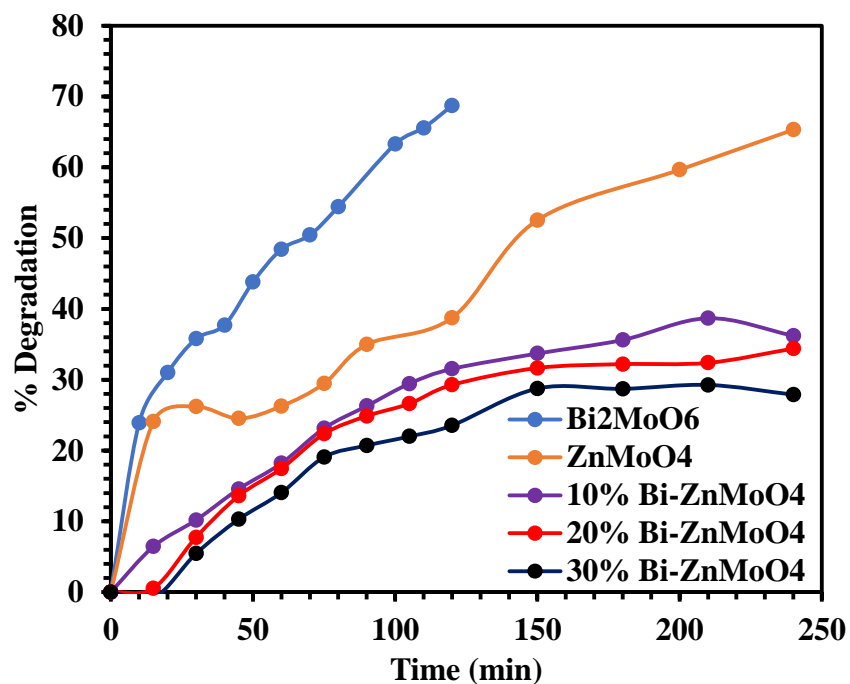


Figure 8: NMP degradation for experiments with PMS 100 mg/l (NMP concentration 10 mg/L, catalyst loading 300 mg/L)

Reaction with PMS 200 mg/L: in this case, 10 mg of PMS were added. Again, the best results were found with the pure Bi₂MoO₆, but this time the 20% Bi₂MoO₆/ ZnMoO₄ also showed good results (60% degradation after 3 hours of reaction) (Fig. 9).

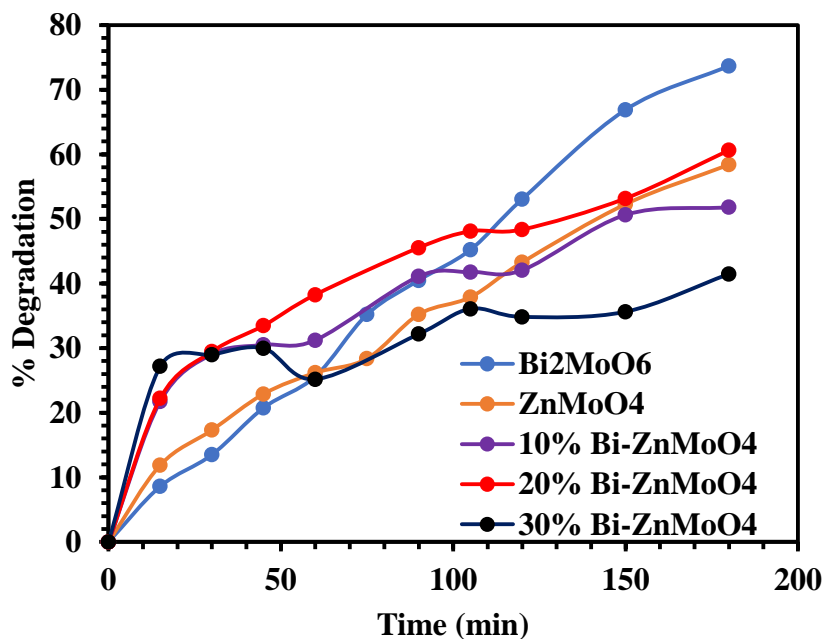


Figure 9: NMP degradation for experiments with PMS 200 mg/L (NMP concentration 10 mg/L, catalyst loading 300 mg/L)

Table 8. Degradation of NMP with 200 mg/L of PMS

Catalyst	Degradation after 3 hours
Bi_2MoO_6	73.7%
ZnMoO_4	58.4%
10% $\text{Bi}_2\text{MoO}_6/\text{ZnMoO}_4$	51.8%
20% $\text{Bi}_2\text{MoO}_6/\text{ZnMoO}_4$	60.6%
30% $\text{Bi}_2\text{MoO}_6/\text{ZnMoO}_4$	41.5%

Reaction with PMS 300 mg/l: to reach this concentration of PMS, 15 mg were added to the 50 mL solution of NMP. Once again, Bi_2MoO_6 caused a higher degradation of NMP, reaching an almost complete degradation in 1 hour, and the catalyst with 20% ratio of $\text{Bi}_2\text{MoO}_6/\text{ZnMoO}_4$ was the best among the composite catalysts. (Fig. 10)

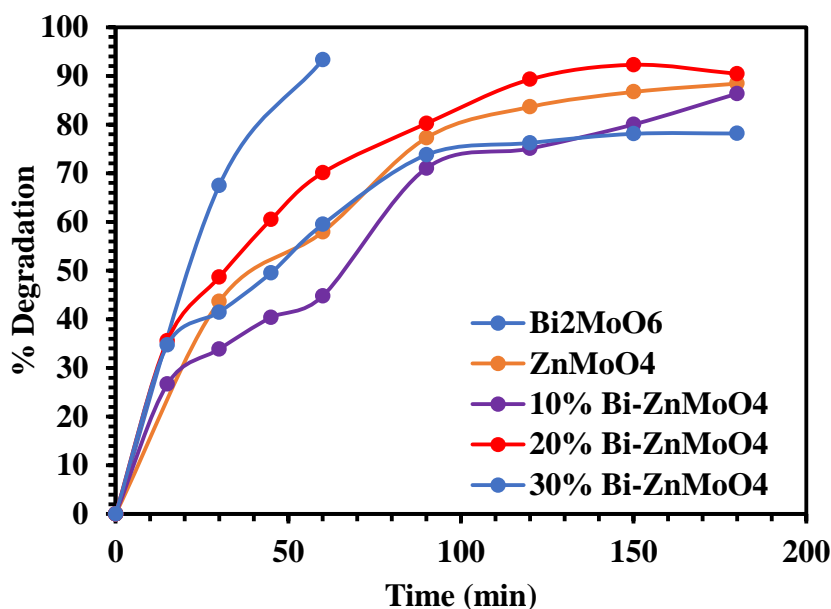


Figure 10: NMP degradation for experiments with PMS 300 mg/l (NMP concentration 10 mg/L, catalyst loading 300 mg/L)

Table 9. Degradation of NMP with 300 mg/L of PMS

Catalyst	Degradation after 3 hours
Bi_2MoO_6	93.31% (1 hour)
ZnMoO_4	88.41%
10% $\text{Bi}_2\text{MoO}_6/\text{ZnMoO}_4$	86.35%
20% $\text{Bi}_2\text{MoO}_6/\text{ZnMoO}_4$	90.42%
30% $\text{Bi}_2\text{MoO}_6/\text{ZnMoO}_4$	78.16%

4.4. Comparison of the effect of PMS concentration for each catalyst

The following graphics (Fig. 11) show the comparison of the NMP degradation for each catalyst, according to the concentration of PMS.

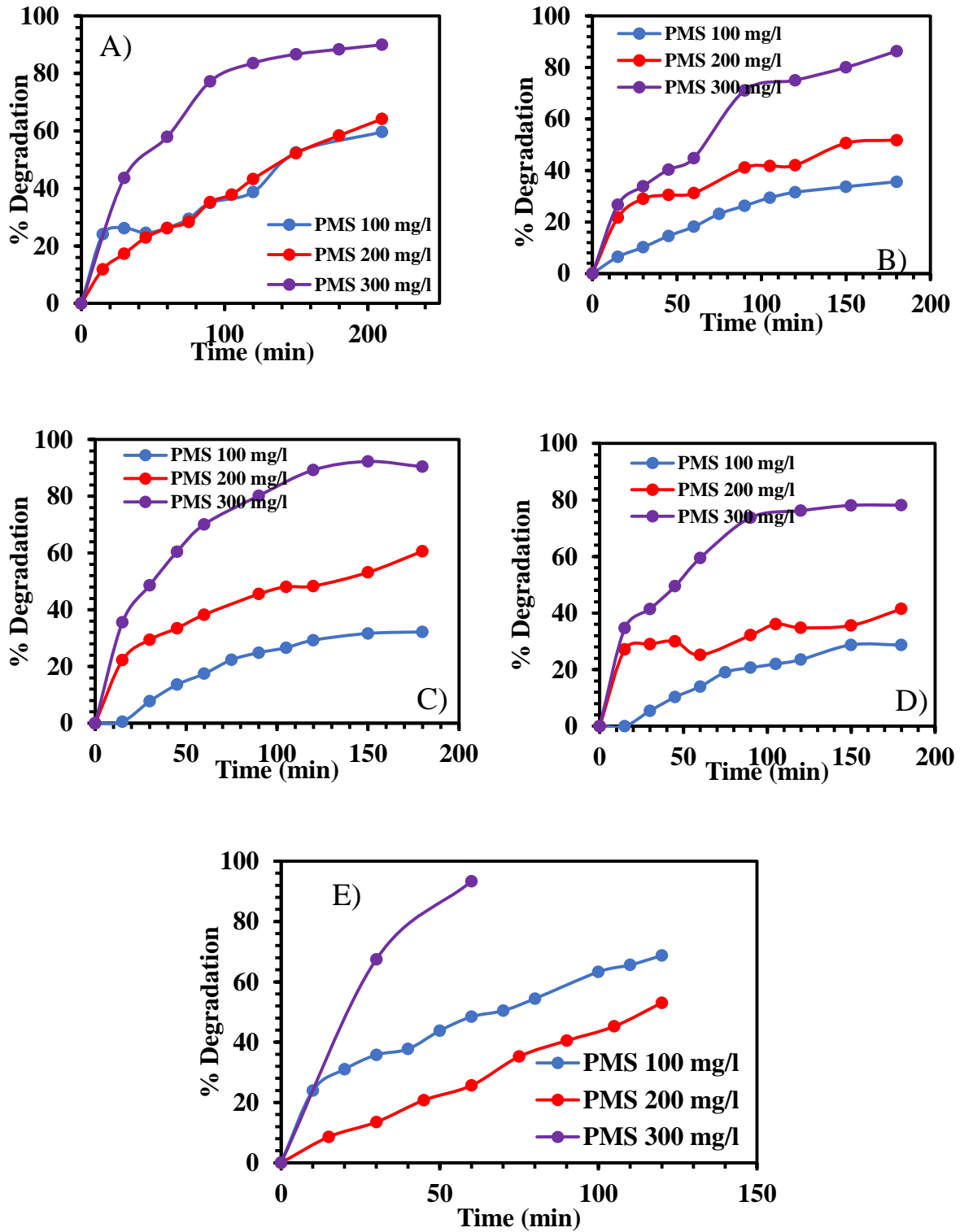


Figure 11: Effect of the PMS concentration for each catalyst. A) ZnMoO_4 ; B) 10% $\text{Bi}_2\text{MoO}_6/\text{ZnMoO}_4$; C) 20% $\text{Bi}_2\text{MoO}_6/\text{ZnMoO}_4$; D) 30% $\text{Bi}_2\text{MoO}_6/\text{ZnMoO}_4$; E) Bi_2MoO_6 . Concentration of catalyst and NMP for every reaction: 300 mg/l and 10 mg/l, respectively

As expected, the higher the concentration of PMS, the higher the degradation of NMP. For every catalyst, a big difference in efficiency is seen between PMS 300 mg/L and the other concentrations studied, meaning that this concentration of PMS is closer to the optimal. For the ZnMoO_4 catalyst, the efficiency of PMS at 100 mg/L and 200 mg/L is virtually the same, while for Bi_2MoO_6 a concentration of 100 mg/l of PMS shows better results than a concentration of 200 mg/L.

4.5. Effect of initial pH

NMP is a polar molecule and liquid at room temperature. When dissolved in water, there is a strong connection between NMP and water molecules through the formation of polymeric species of the type $(\text{NMP}\cdot 2\text{H}_2\text{O})_n^-$. This occurs because of the two lone electrons pairs on the oxygen atom of the carbonyl group of the NMP.

The initial pH of the NMP solution was 6.2, and two more tests were made with lower pH (4.6) and higher pH (9.5), using 1M H_2SO_4 and 1M NaOH to adjust the pH of the solution. For these experiments, the concentration of NMP was 10 mg/L, the PMS concentration was 300 mg/L and that of the photocatalyst was also 300 mg/L.

The photocatalyst chosen for these experiments was the one with 20% ratio of $\text{Bi}_2\text{MoO}_6/\text{ZnMoO}_4$, as this compound had shown good results with the initial NMP solution.

The results are shown in (Fig. 12). Higher pH shows very similar results of those of the initial NMP solution, while with lower pH, the NMP degradation after 4 hours decreases almost 18%.

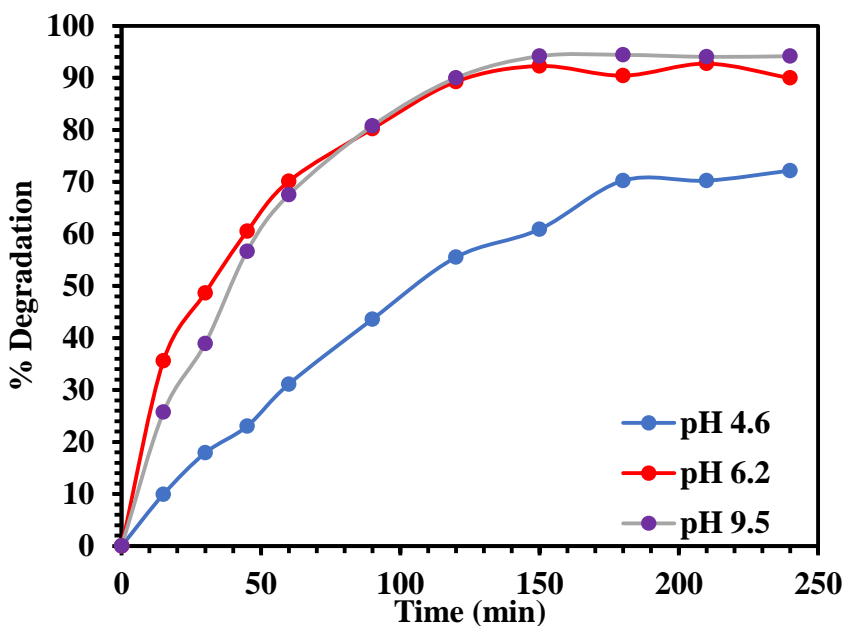


Figure 12: Effect of initial pH on the NMP degradation. (PMS concentration 300 mg/L, catalyst loading 300 mg/L, NMP concentration 10 mg/L)

4.6. Effect of NMP concentration

Some experiments were made using higher concentration of NMP to verify how much of the contaminant is possible to degrade. For this, the photocatalyst used was the 20% $\text{Bi}_2\text{MoO}_6/\text{ZnMoO}_4$, for the same reasons as explained above. The concentration of catalyst and of PMS were 300 mg/L, while the concentration of NMP was changed to 30 mg/l and 40 mg/L. For the initial NMP concentration of 10 mg/L, the results were found quite satisfactory, reaching a maximum degradation rate of 92% after 3 hours. However, with higher concentration of NMP, the degradation showed to be far slower. (Fig. 13)

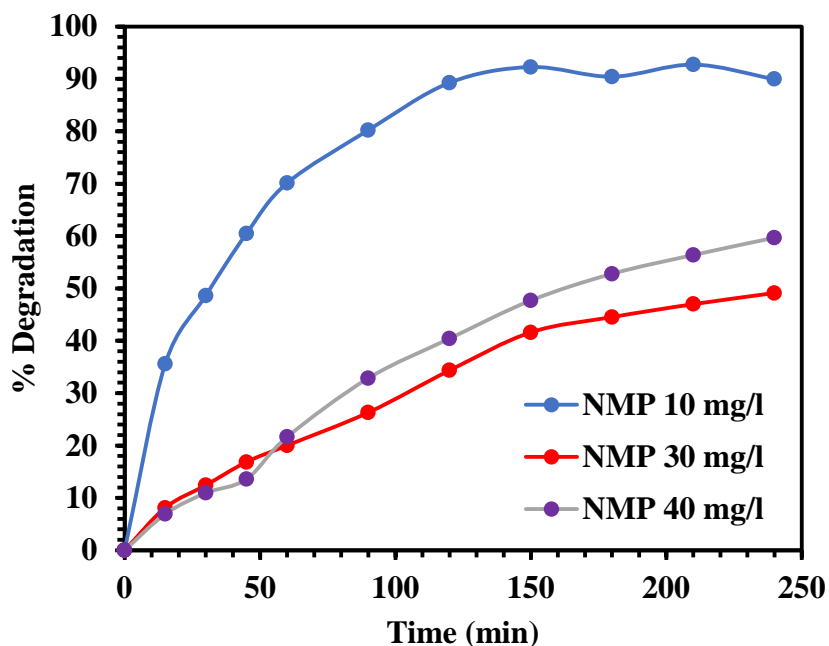


Figure 13: Results of the experiments with different concentrations of NMP. (PMS concentration 300 mg/l, catalyst loading 300 mg/l).

4.7. Effect of UV light

Also, a fast experiment (reaction of only 1 hour) was made for each synthesized photocatalyst, without using any UV light to activate the PMS. For this reason, no PMS was added, and the concentration of catalyst and NMP were 300 mg/L and 10 mg/L, respectively.

Another experiment was done using the 20% Bi₂MoO₆/ ZnMoO₄, but also adding 15 mg of PMS (concentration 300 mg/l) without any source of light. Again, no degradation was found.

For all of these experiments, no degradation of NMP was found, confirming that, without UV activation and PMS, the hydroxyl and sulfate radicals needed for the oxidation process cannot be generated for the degradation to happen.

5. Conclusions

The Bi₂MoO₆/ZnMoO₄ composite photocatalysts were successfully prepared by a modified hydrothermal method and the structural properties were investigated. As shown by the XRD analysis, the crystallite size was smaller in the composites, compared to the single catalysts.

The degradation of NMP with UV-C activated PMS was investigated in this study. The photocatalytic activity of the different catalysts was analyzed, getting different results. Overall, the results with the Bi₂MoO₆ catalyst were found to be the best of all, being possible to reach a degradation higher than 90%. Also, the 20% Bi₂MoO₆/ZnMoO₄ was found to be effective, the best among the composite catalysts. For the PMS concentration, there wasn't a big difference between 100 mg/L and 200 mg/L, but with 300 mg/L it was possible to achieve a much higher degradation of the NMP.

The effect of pH was studied as well, giving better results in native or basic conditions than acidic. No degradation was found without the activation of PMS through UV radiation. For the NMP concentration, it was shown that higher concentrations require far longer times for the NMP degradation to happen, while for the initial concentration of 10 mg/l, it was generally possible to get high degradation rates in only 3-4 hours, or even time with the Bi₂MoO₆ catalyst.

6. References

- [1] Safety Data Sheet of NMP. Accessed on April 1, 2022 <https://www.alfa.com/es/msds/?language=EE&subformat=CLP1&sku=A12260>
- [2] Kumar, P., Verma, S., Kaur, R., Papac, J., Kušić, H., & Štangar, U. L. (2022). Enhanced photo-degradation of N-methyl-2-pyrrolidone (NMP): Influence of matrix components, kinetic study and artificial neural network modelling. **Journal of Hazardous Materials**, *434*, 128807.
- [3] "[Production of batteries made cheaper and safer, thanks to Finnish researchers](#)". **Science Daily**. (Accessed April 1 2022).
- [4] <https://echa.europa.eu/es/substance-information/-/substanceinfo/100.011.662> (Accessed on April 4 2022)

- [5] Růžička, J., Fusková, J., Křížek, K., Měrková, M., Černotová, A., & Smělík, M. (2016). Microbial degradation of N-methyl-2-pyrrolidone in surface water and bacteria responsible for the process. **Water Science and Technology**, 73(3), 643-647.
- [6] Solís-González, C. J., Domínguez-Malfavón, L., Vargas-Suárez, M., Gaytán, I., Cevallos, M. Á., Lozano, L., ... & Loza-Tavera, H. (2017). Novel metabolic pathway for N-methylpyrrolidone degradation in *Alicyclophilus* sp. strain BQ1. **Applied and Environmental Microbiology**, 84(1), e02136-17.
- [7] Cai, S., Cai, T., Liu, S., Yang, Q., He, J., Chen, L., & Hu, J. (2014). Biodegradation of N-methylpyrrolidone by *Paracoccus* sp. NMD-4 and its degradation pathway. **International Biodeterioration & Biodegradation**, 93, 70-77.
- [8] Loh, C. H., Wu, B., Ge, L., Pan, C., & Wang, R. (2018). High-strength N-methyl-2-pyrrolidone-containing process wastewater treatment using sequencing batch reactor and membrane bioreactor: A feasibility study. **Chemosphere**, 194, 534-542..
- [9] Ma, D., Yi, H., Lai, C., Liu, X., Huo, X., An, Z., ... & Yang, L. (2021). Critical review of advanced oxidation processes in organic wastewater treatment. **Chemosphere**, 275, 130104.
- [10] Ma, D., Yi, H., Lai, C., Liu, X., Huo, X., An, Z., ... & Yang, L. (2021). Critical review of advanced oxidation processes in organic wastewater treatment. **Chemosphere**, 275, 130104.
- [11] Liu, C., & Wu, B. (2018). Sulfate radical-based oxidation for sludge treatment: a review. **Chemical Engineering Journal**, 335, 865-875.
- [12] Loures, C. C., Alcântara, M. A., Izário Filho, H. J., Teixeira, A. C. S. C., Silva, F. T., Paiva, T. C., & Samanamud, G. R. (2013). Advanced oxidative degradation processes: fundamentals and applications. **International Review of Chemical Engineering**, 5(2), 102-120.
- [13] Cai, C., Zhang, H., Zhong, X., & Hou, L. (2015). Ultrasound enhanced heterogeneous activation of peroxymonosulfate by a bimetallic Fe–Co/SBA-15 catalyst for the degradation of Orange II in water. **Journal of hazardous materials**, 283, 70-79.
- [14] Xia, X., Zhu, F., Li, J., Yang, H., Wei, L., Li, Q., ... & Zhao, Q. (2020). A review study on sulfate-radical-based advanced oxidation processes for domestic/industrial wastewater treatment: degradation, efficiency, and mechanism. **Frontiers in Chemistry**, 1092.
- [15] Wang, J., & Wang, S. (2018). Activation of persulfate (PS) and peroxymonosulfate (PMS) and application for the degradation of emerging contaminants. **Chemical Engineering Journal**, 334, 1502-1517.
- [16] Yang, S., Wang, P., Yang, X., Shan, L., Zhang, W., Shao, X., & Niu, R. (2010). Degradation efficiencies of azo dye Acid Orange 7 by the interaction of heat, UV and anions with common oxidants: persulfate, peroxymonosulfate and hydrogen peroxide. **Journal of hazardous materials**, 179(1-3), 552-558.
- [17] Chen, Y., Li, M., Tong, Y., Liu, Z., Fang, L., Wu, Y., ... & Huang, L. Z. (2019). Radical generation via sulfite activation on NiFe₂O₄ surface for estriol removal: Performance and mechanistic studies. **Chemical Engineering Journal**, 368, 495-503.
- [18] Shi, P., Su, R., Wan, F., Zhu, M., Li, D., & Xu, S. (2012). Co₃O₄ nanocrystals on graphene oxide as a synergistic catalyst for degradation of Orange II in water by

advanced oxidation technology based on sulfate radicals. **Applied Catalysis B: Environmental**, *123*, 265-272.

[19] Sanchez-Polo, M., Abdel daiem, M.M., OcampoPerez, R., RiveraUtrilla, J., Mota, A.J., 2013. Comparative study of the photodegradation of Bisphenol A by HO·, SO₄⁻ and CO₃/HCO₃ radicals in aqueous phase. **Science of the total environment** 463-464, 423-431

[20] Yoon, S. H., Jeong, S., & Lee, S. (2012). Oxidation of bisphenol A by UV/S₂O₈: Comparison with UV/H₂O₂. **Environmental technology**, *33*(1), 123-128.

[21] Sharma, J., Mishra, I. M., & Kumar, V. (2015). Degradation and mineralization of Bisphenol A (BPA) in aqueous solution using advanced oxidation processes: UV/H₂O₂ and UV/S₂O₈²⁻ oxidation systems. **Journal of environmental management**, *156*, 266-275.

[22] Feng, Y., Song, Q., Lv, W., & Liu, G. (2017). Degradation of ketoprofen by sulfate radical-based advanced oxidation processes: kinetics, mechanisms, and effects of natural water matrices. **Chemosphere**, *189*, 643-651.

[23] Kumar, P., Verma, S., Korošin, N. Č., Žener, B., & Štangar, U. L. (2021). Increasing the photocatalytic efficiency of ZnWO₄ by synthesizing a Bi₂WO₆/ZnWO₄ composite photocatalyst. **Catalysis Today**, *397-399*, 278-285

[24] Zhang, J., Zhou, P., Liu, J., & Yu, J. (2014). New understanding of the difference of photocatalytic activity among anatase, rutile and brookite TiO₂. **Physical Chemistry Chemical Physics**, *16*(38), 20382-20386..

[25] Hojamberdiev, M., Katsumata, K. I., Morita, K., Bilmes, S. A., Matsushita, N., & Okada, K. (2013). One-step hydrothermal synthesis and photocatalytic performance of ZnWO₄/Bi₂WO₆ composite photocatalysts for efficient degradation of acetaldehyde under UV light irradiation. **Applied Catalysis A: General**, *457*, 12-20.

[26] Fifere, N., Airinei, A., Timpu, D., Rotaru, A., Sacarescu, L., & Ursu, L. (2018). New insights into structural and magnetic properties of Ce doped ZnO nanoparticles. **Journal of Alloys and Compounds**, *757*, 60-69.

[27] Jayachandraiah, C., & Krishnaiah, G. (2017). Influence of cerium dopant on magnetic and dielectric properties of ZnO nanoparticles. **Journal of Materials Science**, *52*(12), 7058-7066.

[28] Sin, J. C., Lam, S. M., Lee, K. T., & Mohamed, A. R. (2013). Photocatalytic performance of novel samarium-doped spherical-like ZnO hierarchical nanostructures under visible light irradiation for 2, 4-dichlorophenol degradation. **Journal of colloid and interface science**, *401*, 40-49.